

This is the accepted manuscript made available via CHORUS. The article has been published as:

Search for the largest two-dimensional aggregates of boron: An ab initio study

Ihsan Boustani, Zhen Zhu, and David Tománek

Phys. Rev. B **83**, 193405 — Published 19 May 2011

DOI: [10.1103/PhysRevB.83.193405](https://doi.org/10.1103/PhysRevB.83.193405)

Search for the largest 2D aggregates of boron: An *ab initio* study

Ihsan Boustani,¹ Zhen Zhu,² and David Tománek^{2,3,*}

¹*Bergische Universität Wuppertal, FB C - Mathematik und
Naturwissenschaften, Gaußstrasse 20, D-42097 Wuppertal, Germany*

²*Physics and Astronomy Department, Michigan State University, East Lansing, Michigan 48824-2320, USA*

³*Centre Européen de Calcul Atomique et Moléculaire (CECAM),
Ecole Polytechnique Fédérale de Lausanne (EPFL), 1015 Lausanne, Switzerland[†]*

(Dated: April 4, 2011)

We use *ab initio* density functional calculations to investigate the structural stability and vibrational spectra of small boron aggregates in different charge states. In search of candidates for the largest stable 2D boron aggregates, we focus on systems with one atom less than B₂₀ clusters with confirmed 3D geometry. Whereas the most stable structural isomer of B₁₉⁻ is two-dimensional, in agreement with experimental results of Huang *et al.* [Nature Chem. **2**, 202 (2010)], the second most stable anionic and the most stable neutral and cationic species form a 3D pyramidal structure that had been missed previously.

PACS numbers: 36.40.Ei, 36.40.Wa, 61.48.De, 81.07.Nb

Boron is a fascinating and challenging element that forms not only solids with icosahedral or tetrahedral subunits, but also intriguing structural arrangements in the nano-domain. Early interest in non-crystalline boron structures beyond icosahedral arrangements began in the eighties with theoretical and experimental studies of small boron clusters. The first mass spectra of boron clusters were obtained by Anderson *et al.*^{1,2}. Abundances of particular cluster sizes in these mass spectra were related to the collision-induced dissociation channels and interpreted according to the presumption that more stable isomers do not fragment easily and also do not react readily with O₂ or N₂O. In another important experimental study, La Placa *et al.*³ obtained mass spectra of boron clusters that were initially created by laser ablation of hexagonal boron nitride, followed by a separation and identification of the charged boron clusters using a time-of-flight technique. All experimental data showed “magic numbers” associated with abundances of cationic boron aggregates with $n = 5, 7, 10, 11$, and particularly with $n = 13$ atoms.

Early theoretical studies of small boron clusters, performed by Anderson², Kato^{4,5} and Kawai⁶, correlated the observed mass abundances with relative stabilities of B_{*n*} clusters containing $2 \leq n \leq 12$ atoms. Publications by Anderson² and Kawai⁶ suggest open icosahedral atomic arrangements as the equilibrium structure, whereas Kato *et al.*⁴ finds 2-dimensional (2D) cyclic or butterfly structures more stable than 3D atomic arrangements. Besides providing contradictory results, these theoretical studies also were unable to identify any trends that would give insight into the experimental data.

Small boron clusters exhibit a unique structural property by preferentially forming planar or quasi-planar atomic arrangements. This unique property was proposed theoretically by Boustani⁷ for the first time and was subsequently confirmed experimentally⁸. Boustani also predicted the existence of boron nanotubes^{9,10}, which were subsequently synthesized^{11,12}. Boustani investigated small boron clusters and postulated the so-called “aufbau principle” for the equilibrium structures of boron. According to this guideline, the most stable boron clusters can be constructed from two basic units, namely a pentagonal pyramidal B₆ unit and a hexagonal pyramidal B₇ unit¹³. Highly stable boron nanostructures such as sheets, nanotubes and fullerenes can easily be formed via this aufbau principle^{14–19}.

The transition from 2D to 3D equilibrium geometries of B_{*n*} clusters has been postulated to occur in the size range $16 < n < 24$ atoms^{20,21}. More recently, a 3D double-ring structure has been reported for the neutral B₂₀ aggregate,^{12,22,23} whereas planar structures have been proposed for the B₁₉[−] cluster²⁴ and B₂₀[−] cluster.^{22,23} In this manuscript we investigate theoretically the structure and relative stability of cationic, neutral and anionic boron aggregates with 19 atoms in search of candidates for the largest neutral and charged boron aggregates with 2D geometry.

Negatively charged B₁₉ aggregates in the gas phase were generated by Huang *et al.*²⁴ by first laser vaporizing a ¹⁰B-enriched disc target in helium ambient. Mass selection of the B₁₉[−] aggregates was achieved using time-of-flight mass spectrometry. The clusters were subsequently characterized using photoelectron spectroscopy at laser photon wavelengths 266 nm ($h\nu = 4.661$ eV) and 193 nm ($h\nu = 6.424$ eV).

The experimental data were interpreted theoretically by determining the optimum geometries, vibrational spectra and vertical detachment energies of B₁₉[−] as well as B₁₉ and B₁₉⁺ aggregates using the Density Functional Theory (DFT), as implemented in the SIESTA code^{25,26}. We used the Local Density Approximation (LDA)²⁷ with the Ceperley-Alder exchange-correlation functional²⁸ as parameterized by Perdew and Zunger²⁹. We described interactions between valence electrons and ions by norm-conserving pseudopotentials³⁰ with separable non-local operators³¹. Atomic orbitals with double- ζ polarization were used to expand the electron wave functions^{25,26} with an energy cutoff of 100 Ry for the real-space mesh. We used the low value of 3 mRy as the confinement energy shift that defines the cutoff radii of the atomic orbitals. Geometry optimization for a large number of plausible candidate geometries was performed without symmetry constraints using the conjugate gradient method. In spite of concerns regarding the adequacy of empirical hybrid exchange-correlation functionals for our systems²⁷, we compared our results for selected structures to numerical values obtained using the B3LYP functional that had nevertheless been applied previously to metallic boron structures³². These comparisons were performed at the 6-311+G* level with the 6-311 + G (2df) basis set, as implemented in the Gaussian 03 code³³.

The optimized geometries of the most stable B₁₉[−] anion clusters, sorted by relative energy, are presented in Fig. 1 and the corresponding vibrational spectra in Fig. 2. Knowing the vibrational modes allowed us to consider the effect of zero-point motion on the stability of the individual isomers. We found that the structural isomers depicted in Fig. 1 are generally stable also for the neutral and cationic clusters, albeit with different energy ordering and a different optimum structure. A comparison of relative energies for the different isomers of B₁₉[−], B₁₉ and B₁₉⁺ is given in Table I.

While searching the configurational space of 19-atom boron aggregates using optimization techniques and exploring soft vibration modes, we encountered a very large number of local minima corresponding to structurally and energetically similar isomers. The large number of locally stable structures witnesses to the capability of boron to bond chemically in many different ways. Since our structure optimization procedure was not restricted by symmetry as it was in previous studies, we found that most optimized structures benefited energetically from symmetry-lowering Jahn-Teller distortions. Our criterion for a stable isomer was that the residual Hellmann-Feynman forces acting on all atoms should vanish and that the force-constant matrix be positive semi-definite. The latter criterion was especially

useful in distinguishing metastable structures that contain imaginary eigenfrequencies from truly stable isomers.

In general, we found it relatively easy to determine the equilibrium structure of the most stable isomers. The complexity of the potential energy surface, which turned out to be rather flat especially in the vicinity of structural optima for the less stable isomers, caused generally a larger challenge. Among the many structures with similar geometries, those discussed here are meaningful representatives of a class of structurally and energetically closely related systems.

Among the data presented in Table I, the most interesting result concerns the energy difference between 2D and 3D structures for different charge states. Whereas the 2D structure (1) with a central rhombus is energetically preferred for the anionic B_{19}^- , we find the 0.05 eV less stable 3D pyramidal structure (2), which had been missed in previous studies,²⁴ an energetically close contender. For the neutral and anionic species the 3D pyramidal structure even turns out as the most stable isomer. Consequently, the 2D–3D transition in the growth pattern of boron structures occurs in 19-atom boron aggregates.

On energetic grounds, we feel that 2D isomers (1) and (3) may coexist with the 3D isomer (2) under synthesis conditions. With the exception of the 3D isomer (2), which has not been discussed previously, our results for the most stable isomers of B_{19}^- agree qualitatively with those of Huang *et al.*²⁴. Whereas the central rhombus structure (1) is preferred by 0.15 eV over the central pentagon structure (3) in our study, calculations of Huang *et al.*²⁴ favor isomer (3) by 0.16 eV over isomer (1). In view of this minor discrepancy in energy ordering, we re-optimized structures (1) and (3) at the level of B3LYP/6-311 G* and found (1) to be favored over (3) by 0.34 eV, confirming our initial energy ordering. The fourth most stable anionic isomer (4) is a quasi-planar or buckled triangular structure composed of dovetail hexagonal pyramids, which is 0.31 eV less stable than the most stable anionic isomer, in qualitative agreement with the results of Huang *et al.*²⁴. Other relatively stable isomers are, in the order of stability for B_{19}^- , the central hexagon structure (5), the double ring structure (6) and the hexagonal vacancy structure (7). Only some of these structures have been discussed previously, with similar reported energy ordering. Our values for the vertical detachment energies, obtained from total energy differences between B_{19}^- and B_{19} in the same frozen geometry, are 4.4 eV for isomer (1) (experimental value²⁴ 4.1 eV) and 4.6 eV for isomer (3) (experimental value²⁴ 4.3 eV) are in reasonably good agreement with the observed data.

As mentioned earlier, symmetry constraints, such as confinement to a planar structure, often increase the ground-state energy. To quantify the energetic benefit associated with buckling in B_{19}^- , we re-optimized the buckled triangular structure (4) by constraining it to a plane. The resulting planar triangular structure turned out to be less stable by 0.12 eV than the optimized structure (4). Even though all forces acting on atoms in the planar structure vanish, the system was found to be metastable, as indicated by the presence of a buckling eigenmode with imaginary frequency of 265 cm^{-1} .

Owing to the naturally occurring isotope abundance of 19.9% ^{10}B and 80.1% ^{11}B , we used the average mass number 10.81 a.m.u. for boron when calculating the vibration spectra in Fig. 2. The 10% mass difference between the two major isotopes will obviously translate to a 5% effect on the vibrational frequencies in isotopically pure clusters, amounting to a typical isotope shift of up to 50 cm^{-1} . Our results in Fig. 2 indicate that the hardest vibrational modes of B_{19}^- occur at $\omega \lesssim 1500\text{ cm}^{-1}$, witnessing to the rigidity of the B-B bond. We find the vibrational spectra of the different isomers to be sufficiently different to allow for spectroscopic identification of the structure. The important role played by hard vibrational modes is reflected also in the zero-point energy, which is close to 2.0 eV for all structures, independent of the charge state. Maximum difference in the zero-point energy of $\lesssim 0.1\text{ eV}$ are not sufficient to change the energy ordering based on the optimum geometry at $T = 0$.

In general, we found that a majority of most stable B_{19}^- isomers follow the general trend indicating that boron prefers to be surrounded by 5 – 6 atoms in a locally planar geometry. A notable exception to this rule is the disordered, low-symmetry 3D pyramidal isomer (2). In all these structures we found the bond lengths to range from 1.5 – 1.9 Å, with an average at $\approx 1.75\text{ Å}$. The large number of structurally very different isomers is a consequence of the fact that boron, as an electron deficient element, is forced to combine two-center two-electron (2c-2e) bonds with three-center two-electron (3c-2e) and multi-center two-electron (mc-2e) bonds.

As suggested above, the equilibrium structure of the neutral B_{19} aggregates is very close to that of the anions, depicted in Fig. 1. The most important difference with regard to the anionic species is the 3D pyramidal structure that is more stable than any 2D isomers. In view of the small energy difference of 0.21 eV between the pyramidal isomer (2) and the central rhombus structure (1), both isomers should coexist under experimental conditions. We also wish to point out that the small energy differences reported for these cluster sizes are often comparable to those found for *ab initio* total energy values obtained using different approximations, which are also of the order $\lesssim 0.2\text{ eV}$. Also in view of the complex bonding chemistry of boron, which makes it very hard to probe the potential energy surface near local minima, structures with energy differences of $\lesssim 0.2\text{ eV}$ should be considered energetically degenerate.

Cationic B_{19}^+ aggregates exhibit many similarities as compared to the neutral species, in particular the 3D pyramidal structure (2) as the most stable isomer. The energy difference of 0.88 eV between this and the second most stable isomer (1) is much more pronounced than in the neutral species, indicating a pronounced preference for a 3D structural

arrangement.

In conclusion, we used *ab initio* density functional calculations to investigate the structural stability of small boron aggregates in different charge states. In search of candidates for the largest 2D boron aggregates, we focused on systems with 19 atoms. This aggregate size is interesting from our viewpoint, since neutral B_{20} clusters have 3D geometry, whereas 2D arrangements have been reported for anionic B_{20}^- clusters. We find a similar situation also for the different charge states of the 19-atom aggregates. Whereas the most stable structural isomer of B_{19}^- is two-dimensional, in agreement with previous experimental results, the second most stable anionic and the most stable neutral and cationic species form a 3D pyramidal structure that had been missed previously. Consequently, the 2D–3D transition in the growth pattern of boron structures occurs in 19-atom boron aggregates.

ACKNOWLEDGMENTS

IB and DT acknowledge the hospitality of CECAM while performing this research and useful discussions with Savas Berber, Young-Kyun Kwon and Rick Becker, who provided initial inspiration for this study. A post-doctoral fellowship for IB and partial financial support for DT was provided by the National Science Foundation Cooperative Agreement #EEC-0832785, titled “NSEC: Center for High-rate Nanomanufacturing”. Computational resources have been provided by the Michigan State University High Performance Computing Center and the Computer Center at the University of Wuppertal.

-
- * E-mail: tomanek@pa.msu.edu
- † Temporary affiliation.
- ¹ L. Hanley, J. Whitten, and S. L. Anderson, *J. Phys. Chem.* **92**, 5803 (1988).
 - ² L. Hanley, and S.L. Anderson, *J. Chem. Phys.* **89**, 2848 (1988).
 - ³ S. J. La Placa, P. A. Roland, and J. J. Wynne, *Chem. Phys. Lett.* **190**, 163 (1992).
 - ⁴ H. Kato, and E. Tanaka, *J. Comput. Chem.* **12**, 1097 (1991).
 - ⁵ H. Kato, K. Yamashita, and K. Morokuma, *Bull. Chem. Soc. Jpn.* **66**, 3358 (1993).
 - ⁶ R. Kawai, and J. H. Weare, *J. Chem. Phys.* **95**, 1151 (1991).
 - ⁷ I. Boustani, *Int. J. Quantum Chem.* **52**, 1081 (1994).
 - ⁸ H.-J. Zhai, B. Kiran, J. Li, and L.S. Wang, *Nature Mater.* **2**, 827 (2003).
 - ⁹ I. Boustani, and A. Quandt, *Europhys. Lett.* **39**, 527 (1997).
 - ¹⁰ I. Boustani, A. Quandt, E. Fernandez, and A. Rubio, *J. Chem. Phys.* **110**, 3176 (1999).
 - ¹¹ D. Ciuparu, R. F. Klie, Y. Zhu, and L. Pfefferle, *J. Phys. Chem. B* **108**, 3967 (2004).
 - ¹² B. Kiran, S. Bulusu, H.-J. Zhai, S. Yoo, X. C. Zeng, and L.-S. Wang, *Proc. Natl. Acad. Sci. U.S.A.* **102**, 961 (2005).
 - ¹³ I. Boustani, *Phys. Rev. B* **55**, 16426 (1997).
 - ¹⁴ H. Tang and S. Ismail-Beigi, *Phys. Rev. Lett.* **99**, 115501 (2007).
 - ¹⁵ A. Y. Liu, R. R. Zope, and M. R. Pederson, *Phys. Rev. B* **78**, 155422 (2008).
 - ¹⁶ N. Gonzalez Szwacki, A. Sadrzadeh, and B. I. Yakobson, *Phys. Rev. Lett.* **98**, 166804 (2007); *ibid.* **100**, 159901 (2008) (E).
 - ¹⁷ R. R. Zope, T. Baruah, K. C. Lau, A. Y. Liu, M. R. Pederson, and B. I. Dunlap, *Phys. Rev. B* **79**, 161403 (2009).
 - ¹⁸ H. Tang and S. Ismail-Beigi, *Phys. Rev. B* **82**, 115412 (2010).
 - ¹⁹ C. Özdoğan, S. Mukhopadhyay, W. Hayami, Z. B. Güvenc, R. Pandey, and I. Boustani, *J. Phys. Chem.* **114**, 4362 (2010).
 - ²⁰ Saikat Mukhopadhyay, Haying He, Ravindra Pandey, Yoke Khin Yap and Ihsan Boustani, *J. Phys.: Conf. Ser.* **176**, 012028 (2009).
 - ²¹ S. Chacko, D. G. Kanhere, and I. Boustani, *Phys. Rev. B* **68**, 035414 (2003).
 - ²² Wei An, Satya Bulusu, Yi Gao, and X. C. Zeng, *J. Chem. Phys.* **124**, 154310 (2006).
 - ²³ Alina P. Sergeeva, Dmitry Yu. Zubarev, Hua-Jin Zhai, Alexander I. Boldyrev, and Lai-Sheng Wang, *J. Am. Chem. Soc.* **130**, 7244 (2008).
 - ²⁴ W. Huang, A. P. Sergeeva, H.-J. Zhai, B. B. Averkiev, L.-S. Wang, and A. I. Boldyrev, *Nature Chem.* **2**, 202 (2010).
 - ²⁵ D. Sánchez-Portal, P. Ordejón, E. Artacho, and J. M. Soler, *Int. J. Quantum Chem.* **65**, 453 (1997).
 - ²⁶ J. M. Soler, E. Artacho, J. D. Gale, A. García, J. Junquera, P. Ordejón, and D. Sánchez-Portal, *J. Phys.: Condens. Matter* **14**, 2745 (2002).
 - ²⁷ We wish to emphasize the superiority of local exchange-correlation functionals in our system to hybrid semi-empirical functionals such as B3LYP, which are notoriously wrong in the description of metallic systems such as boron nanostructures, since they fail to describe correctly systems with uniform electron density.
 - ²⁸ D. M. Ceperley and B. J. Alder, *Phys. Rev. Lett.* **45**, 566 (1980).
 - ²⁹ J. P. Perdew and A. Zunger, *Phys. Rev. B* **23**, 5048 (1981).
 - ³⁰ N. Troullier and J. L. Martins, *Phys. Rev. B* **43**, 1993 (1991).
 - ³¹ L. Kleinman and D. M. Bylander, *Phys. Rev. Lett.* **48**, 1425 (1982).
 - ³² E. Oger, N. R. M. Crawford, R. Kelting, P. Weis, M. M. Kappes, and R. Ahlrichs, *Angew. Chem. Int. Ed.* **46**, 8503 (2007).
 - ³³ M. J. Frisch et al., Computer code GAUSSIAN 03, revision B.03, Gaussian, Inc., Wallingford, CT (2004).

FIGURES

FIG. 1. (Color online) Equilibrium geometry and total energy differences, corrected for zero-point energies, between different structural isomers of B_{19}^- anion clusters. For selected structures, the varying degree of planarity is depicted in top and side view.

FIG. 2. Vibrational spectra of stable B_{19}^- isomers, convoluted with a 50 cm^{-1} FWHM Gaussian function. The labeling of the structural isomers follows Fig. 1.

TABLES

TABLE I. Relative energies of B_{19} neutral, B_{19}^- anion and B_{19}^+ cation clusters. Total energy differences contain zero-point motion corrections. The labeling of the structural isomers follows Fig. 1.

Isomer identification	$\Delta E(B_{19}^-)$ (eV)	$\Delta E(B_{19})$ (eV)	$\Delta E(B_{19}^+)$ (eV)
(1) Central rhombus	0.00	0.21	0.88
(2) Pyramid	0.05	0.00	0.00
(3) Central pentagon	0.15	0.76	1.99
(4) Buckled triangular	0.31	0.62	1.54
(5) Central hexagon	1.07	0.61	0.89
(6) Double ring	1.67	0.85	0.95
(7) Hexagonal vacancy	1.92	1.80	2.47

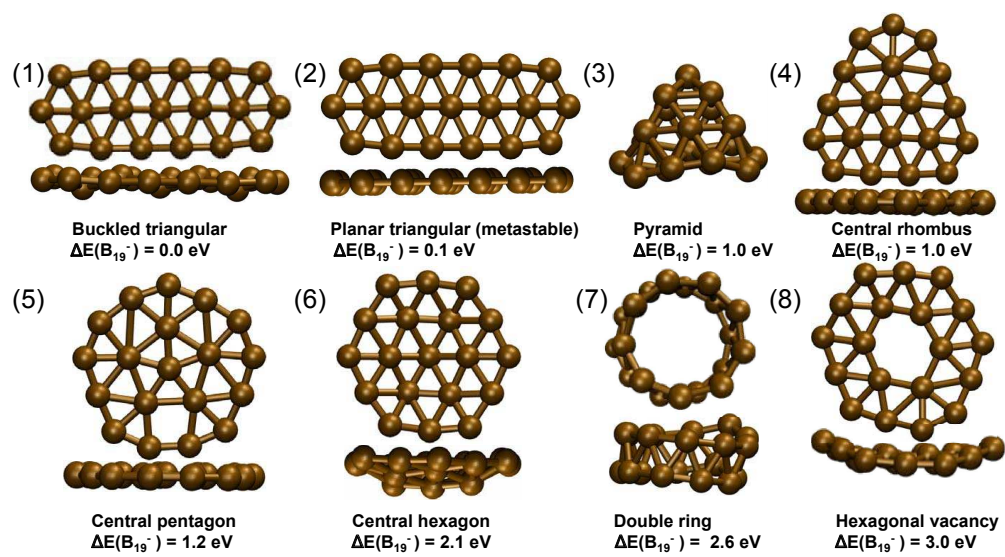


Figure 1

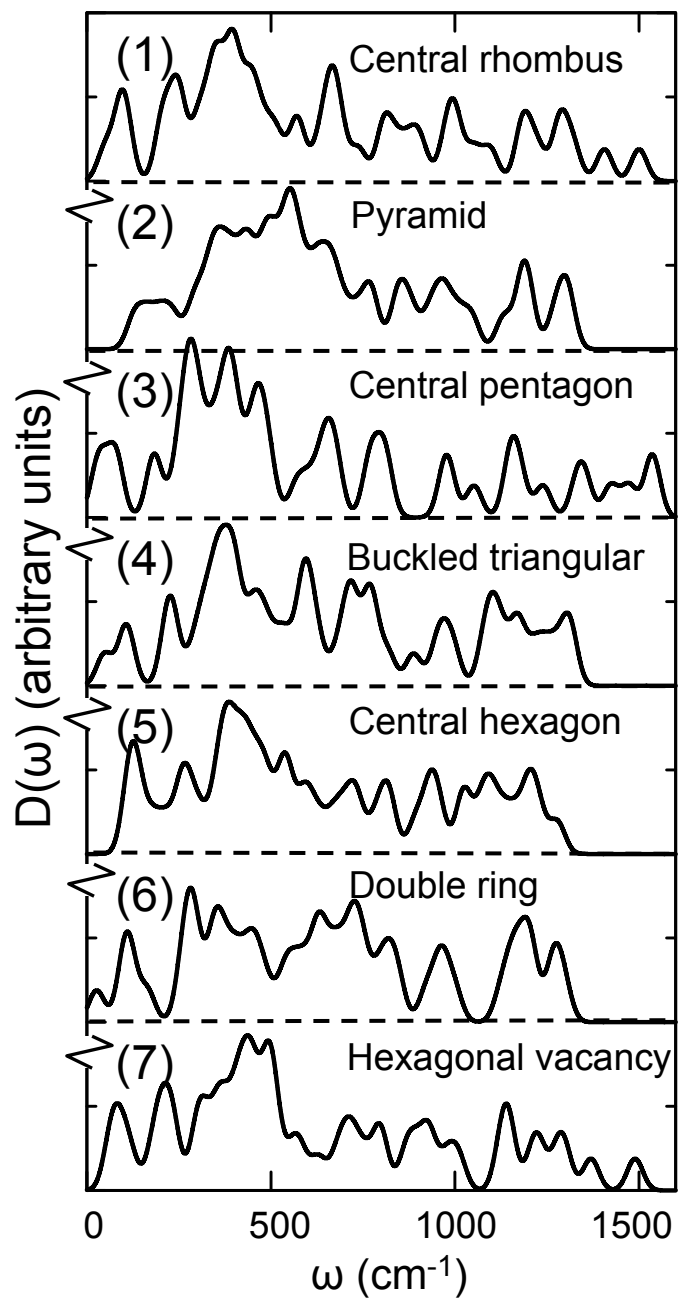


Figure 2 BUJ1139 04Apr2011